Chapter 4

Evolutionary cohorts or individual species?

A comparative phylogeography case study

This chapter is being prepared for journal submission as "Evolutionary cohorts or individual species? A comparative phylogeography case study using five New Zealand forest beetles" by Marske, K.A., Leschen, R.A.B. & Buckley, T.R. I was responsible for the conception, design and execution of the research and for writing the manuscript. Thomas Buckley and Richard Leschen assisted with conception and design, insect collecting and manuscript editing. Sequence data will be made available via GenBank following publication of the manuscript.

Chapter Summary: Phylogeographic structure and its underlying causes are not necessarily shared among community members, with important implications for using individual organisms as indicators for ecosystem evolution, such as the identification of forest refugia. Over 1000 mtDNA (COI) sequences and newly developed coalescent phylogeography models were used to construct geo-spatial histories for five co-distributed New Zealand forest beetles. These methods utilize continuous-time Markov chains and Bayesian stochastic search variable selection (BSSVS) to identify historical dispersal patterns and migration matrices via ancestral state reconstruction. We also used ecological niche models to reconstruct the potential geographic distribution of each species during the Last Glacial Maximum (LGM). Results for all five species yielded a complex picture of temperate forest community evolution, with each species sharing some results with every other, but no general patterns were detected among all five. Shared LGM forest refugia were detected near Karamea, between Nelson and Marlborough, at Kaikoura and near the Haast River mouth. These results indicate that

forest species retreated into and expanded out from the same refugia by a variety of routes, rather than travelling together as an intact forest community.

4.1 Introduction

Comparative phylogeography seeks to understand ecosystem evolution by identifying shared responses to historical events among disparate taxa (Bermingham & Moritz 1998). Of particular emphasis has been where species from a variety of habitats survived the late-Pleistocene Last Glacial Maximum (LGM), which had a major influence on the distribution of the global biota, and how they expanded from these glacial refugia to fill their modern distributions (Waltari *et al.* 2007). For some systems, particularly in the Northern Hemisphere, enough phylogeographic data have accumulated to inform consensus on broad regional patterns of biogeography and evolution (e.g., Hewitt 2000), detect different historical trajectories among co-distributed species (e.g., Soltis *et al.* 2006), and utilize well-known empirical systems for developing and testing new phylogeographic methods (e.g., Richards et al. 2007).

These methodological developments are fairly recent, yet phylogenies have been used to investigate phylogeography for the last 20 years (Avise *et al.* 1987; Hewitt 2000; Hickerson *et al.* 2010). Synthesizing studies of glacial refugia identified "characteristic" patterns of species response to Pleistocene climate change, such as the well-known "southern richness, northern purity" distribution of genetic diversity in heavily-glaciated regions of the northern hemisphere (Hewitt 2000). However, a growing body of data suggest that the latitudinal retreat paradigm is an over-simplification, with the biomes of each geographic region subject to different environmental and topographic pressures, resulting in different patterns (Soltis *et al.*

2006). Even in Europe, upon which this paradigm was largely based, increasing evidence exists for the role of northern refugia in postglacial colonization of the flora and fauna (e.g., Bhagwat & Willis 2008; Dépraz *et al.* 2008; Gratton *et al.* 2008), and for fragmentation of the southern peninsular refugia into discrete areas of endemism and absence (e.g., Canestrelli *et al.* 2007; Centeno-Cuadros *et al.* 2009; Previšić *et al.* 2009).

Pleistocene conditions in the Northern Hemisphere were extremely different from those in the temperate south, where the Pleistocene Last Glacial Cold Period began earlier and lasted longer than the global LGM (Woodward & Shulmeister 2007) and overlaid recent tectonic activity, volcanism and landscape evolution (Rabassa & Clapperton 1990; King 2000; Alloway *et al.* 2007). First, South America and New Zealand experienced montane and valley glaciation, rather than major ice shields (Rabassa & Clapperton 1990; Hulton *et al.* 2002; Suggate & Almond 2005). As a result, the habitability of landscapes was determined by factors like extreme weather and drought, rather than the cold associated with extensive ice sheets (Markgraf *et al.* 1995; Drost *et al.* 2007). Second, glaciers were not separated from temperate zones by an extensive tundra belt, as in the Northern Hemisphere, and evidence suggests some temperate species were able to survive in close proximity to glaciers (Shepherd *et al.* 2007; Marra & Thackray 2009). Third, Pleistocene sea level fluctuation resulted in significant increases to the southern landmasses, and studies suggest that this exposed continental shelf was more important for glacial refugia than many modern terrestrial areas (e.g., Alloway et al. 2007). For New Zealand, a growing body of evidence exists for temperate forest refugia outside of those indicated by a recent synthesis of fossil and sediment data, including in the higher latitudes of the South Island (Alloway et al. 2007; Shepherd *et al.* 2007; Leschen *et al.* 2008; Buckley *et al.* 2009; Marshall *et al.* 2009).

Data syntheses from other regions indicate that phylogeographic structure in co-distributed taxa, as well as the causes underlying the observed genetic structure, can be complex (e.g., Soltis *et al.* 2006). Sullivan et al. (2000) found that species shifted neither completely independently in response to glacial cycles, nor as a fully intact community. Carstens *et al.* (2005) subsequently observed that looking for genetic concordance among co-distributed species assumes they were co-distributed in the past, but that this hypothesis is rarely tested. Following in this vein, Soltis *et al.* (2006) highlighted the issue of pseudo-congruence, in which spatially similar genetic patterns are generated at different times by different causes, or where subtly different spatial patterns are misinterpreted as identical. Applications of coalescent methods and ecological niche models (ENMs) have identified specific instances of these issues: Carstens & Richards (2007) detected congruent phylogeographic patterns and similar modern distributions in species from different ancestral refugia, while Leaché *et al.* (2007) inferred different time scales for a "common" phylogeographic barrier, implying multiple vicariant events driving similar population structure across the same region. To understand the biogeography of an ecosystem, not just the individual taxa inhabiting it, these results emphasize the need for rigorous phylogeographic methods, validation of assumptions of ancestral congruence (such as ENMs or fossils), and comparative studies across a broad spectrum of available taxa (e.g., Carstens & Richards 2007). For geologically and ecologically complex regions, where the landscape and its biota are sculpted by a variety of events overlying each other in space and time, extensive sampling of species' geographic distributions is especially important (Hedin & Wood 2002; Turner *et al.* 2009).

This chapter will address the difference between the biogeography of an ecosystem and those of its constituent species. New Zealand is an ideal setting for

comparative phylogeography and evolutionary studies because of its recent turbulent geological history, in which Pleistocene glaciation overlaid significant tectonic reorganization of the landscape and uplift of the major mountain ranges, largely crowded into the last 10 Ma (King 2000; Pulford & Stern 2004; Naish 2005; Bunce *et al.* 2009). Utilizing the temperate lowland forests of New Zealand, we will address whether five co-distributed forest beetles from similar microhabitats comprise an "evolutionary cohort", a group of species which track environmental changes together through time (Carstens & Richards 2007), or whether climate change response is more species-specific in nature, and how this relates to climatic response of the forest as a whole. Newly developed coalescent phylogeography methods and ecological niche models will be implemented to 1) identify LGM forest refugia utilized by each species; 2) assess congruence among phylogenies, ENMs and patterns of gene flow within and among species; and 3) evaluate how the histories of individual species relate to that of the forest community as a whole. We will also address how projected refugia and patterns of gene flow relate to the South Island refugium at Karamea detected by Alloway et al. (2007).

4.2 Methods

4.2.1 Sampling

Focal taxa include *Agyrtodes labralis* (Broun) (Leiodidae), *Brachynopus scutellaris* (Redtenbacher) (Staphylinidae), *Epistranus lawsoni* (Sharp) (Zopheridae) and *Pristoderus bakewelli* (Pascoe) (Zopheridae). All occur in dead wood and leaf litter feeding on fungi and require the presence of forest established long enough to have

generated woody debris and fungal ecosystems, but are not limited to a specific wood type. The fifth species, *Hisparonia hystrix* (Sharp) (Nitidulidae), is an arboreal feeder on sooty moulds, which grow primarily on southern beech (*Nothofagus* spp.; Nothofagaceae) and manuka (*Leptospermum scoparium* Forst. & Forst.; Myrtaceae) trees fed upon by honey-dew secreting scale insects (Carlton & Leschen 2007), and is present in scrub and forest margin habitats as well as tall forest. *Brachynopus scutellaris*, *E. lawsoni*, *H. hystrix* and *P. bakewelli* are widely distributed throughout New Zealand, although *B. scutellaris* is absent from the Westland *Nothofagus* gap, an area of the South Island's west coast across which the distribution of *Nothofagus* is disjunct (Löbl & Leschen 2003; Leschen *et al.* 2008), and *A. labralis* is absent from the North Island (Seago 2009). Detailed collecting methods for *A. labralis, E. lawsoni* and *P. bakewelli* are described in Chapters 2-3. Specimens of *B. scutellaris* were collected by hand directly from over-turned pieces of wood, or by crumbling, sifting and subjecting woody debris to Berlese or Winkler funnel extraction. *Hisparonia hystrix* were collected by beating vegetation or rubbing tree trunks covered with sooty mould. All specimens were collected directly into 95% ethanol and stored at -20º C. GIS locality information was recorded for each collection site.

4.2.2 Ecological niche modelling

Ecological niche models were generated for *A. labralis*, *B. scutellaris* and *H. hystrix* using the methods described for *E. lawsoni* and *P. bakewelli* (Chapter 3). Briefly, climate variables for current and LGM projections included mean annual rainfall (mm), mean February rainfall (mm), mean annual solar radiation (kJ/day/m^2), mean annual temperature (°C), mean February temperature (°C), minimum temperature

of the coldest month (°C, July), and October vapour pressure deficit (kPa) (Leathwick *et al.* 1998; Leathwick *et al.* 2003). LGM (c. 22,000 cal. yr BP) projections were based on estimates of temperature depression from marine isotope stages and estimates of LGM topography obtained by extending the modern DEM down to the 120m bathymetry (J.R. Leathwick, unpublished data). Ecological niche models were generated in Maxent 3.3.1 (Phillips *et al.* 2006; Phillips & Dudík 2008), and were subject to 10-fold cross-validation to ensure consistency of model predictions and ecological variable response among repeated runs. Model performance was evaluated using the threshold-dependent binomial omission tests and the Area Under the (Receiver Operating Characteristic; ROC) Curve (AUC) calculated by Maxent. To ensure that significant AUCs represented true difference from random, null models were developed to compare our species' model performance against points randomly drawn from all of New Zealand, and from areas of New Zealand with native forest cover. The final geographical projections represent the mean point-wise probability of presence over ten model runs applied to modern and LGM environmental layers.

Localities for *A. labralis* were the same (91) as in Chapter 2, with modeling repeated to ensure consistency of methods among species. For *B. scutellaris* and *H. hystrix*, 139 and 134 localities were used, respectively. The current distributions of *A. labralis, B. scutellaris* and *E. lawsoni* were also modelled with the addition of three vegetation layers, *Nothofagus* spp., Podocarpaceae and Myrtaceae (all in stems/hectare) (Leathwick 1998; Leathwick & Austin 2001) to assess the relationship between *B. scutellaris* and *Nothofagus* spp.

4.2.3 DNA sequencing and sequence statistics

Genomic DNA was extracted from 227 *B. scutellaris* and 203 *H. hystrix* from the North, South and Stewart Islands. Total genomic DNA extraction, purification and sequencing followed the protocols in Chapter 2. Amplification was conducted under PCR conditions in Leschen *et al.* (2008), from which data were incorporated in the genetic analyses; this included 113 and 105 individuals of *B. scutellaris* and *H. hystrix*, respectively (GenBank Accession numbers EU145025-EU145243). Population statistics, including haplotype diversity and Tajima's *D* and Fu and Li's *F** and *D** tests for selective neutrality, were calculated using DnaSp 5.0 (Rozas *et al.* 2003). Base pair differences between sequences were calculated in MEGA 4 (Tamura *et al.* 2007).

4.2.4 Coalescent phylogenetic and molecular clock analyses

The best-fit model of sequence evolution was determined for *B. scutellaris* and *H. hystrix* using the AIC, implemented in Modeltest 3.7 (Posada and Crandall 1998) and PAUP*4.0b10 (Swofford 2003). This yielded GTR+I+Γ for *B. scutellaris* and K81uf+I+Γ for *H. hystrix*. Molecular clock analyses were conducted in BEAST 1.4.8 (Drummond & Rambaut 2007) under a Bayesian coalescent framework. I used Brower's (1994) rate of invertebrate mitochondrial DNA evolution of 0.0115 substitutions/ site from the root to the tips of the tree. MCMC simulations were performed using a strict molecular clock, under both the constant size and exponential growth population models. BEAST profiles incorporated a UPGMA starting tree and the following priors: transition/transversion rate ratio (Jeffrey's), alpha parameter for among-site rate variation (exponential, mean = 10), proportion of invariable sites (uniform, 0-1), clock rate (normal; mean 0.0115, sd 0.00115), and population size

(exponential, mean=1.0). Under the constant size model, root height (exponential, mean=1.0) were used. Under the exponential growth model, coalescent growth rate (uniform) and tree prior (exponential, mean=1.0) were used. Each profile ran ten times for 50 million generations, logging every 2000 generations, and log files from each set of runs were combined using LogCombiner (Drummond & Rambaut 2007), which were then imported into Tracer 1.4 (Rambaut & Drummond 2007) to calculate Bayes Factors (Newton & Raftery 1994) to compare the constant size and exponential growth models for each species. Individual tree files were reduced in size (burnin=6250, thinning interval=5000) and then combined (thinning interval 4000) using LogCombiner and TreeAnnotator (Drummond & Rambaut 2007) to yield a consensus tree for each set of analyses.

4.2.5 Coalescent phylogeographic reconstruction

Phylogeographic relationships between tree tip localities were estimated using the continuous-time Markov chains (CTMCs) and Bayesian stochastic search variable selection (BSSVS) applications in BEAST 1.5.2 and 1.5.3, which incorporate sampling locations as prior probability specifications to reconstruct dispersal patterns inherent in a species' evolutionary history (Lemey *et al.* 2009). Geographic locations are inferred as "states", which are mapped across the time-scaled phylogeny as an ancestral state reconstruction using the CTMCs. The BSSVS allows simultaneous inference of ancestral locations and detection of non-zero rates of state-transition (location change), and state-pairs with statistically significant non-zero rates can be identified using Bayes factors. Significant non-zero rates between locations indicate likely migratory

pathways, in which flow is assumed bidirectional rather than one-way (Lemey *et al.* 2009).

Phylogeographic histories were simulated for each species using coalescent parameters as previously described (above, Chapters 2-3), with the addition of exponential geographic priors after Lemey *et al.* (2009). Geographic regions inferred as "states" were informed by areas projected as common refugia or uninhabited zones in the ENMs and were used for all species to facilitate comparison, although for *A. labralis*, an additional Westland region was incorporated, and for *P. bakewelli*, the single Taranaki sequence was included in Manawatu. Tree files from five runs were combined to generate a consensus tree for each species, and were formatted for visualization of the temporal dynamics of spatial diffusion in Google Earth (http://earth.google.com) (Lemey *et al.* 2009); these have been summarized in ArcGIS. State probabilities for the root were ranked to identify states in the lowest 5%. Discrete rate matrices from all five runs were combined, and a Bayes factor test (script available at BEAST website) was applied to the non-zero rates, with Bayes factor >3.0 indicating well-supported diffusion rates between states (regions).

4.3 Results

4.3.1 Ecological niche models

Bioclimatic models of the distribution of *B. scutellaris* were able to detect presence significantly better than random predictions. The 10-fold cross-validation runs yielded an average AUC of 0.831 (sd 0.079, range 0.7255-0.9057) and performed significantly better than random across most thresholds and runs, although the lower thresholds were not significant for some runs. Jackknife tests of variable importance,

averaged across all runs, were positive for training gain, test gain and AUC. Heuristic estimation of relative contributions of the environmental variables to the Maxent model ranked them as follows: February temperature (25.8%), annual temperature (22.7%), October vapour pressure deficit (13.7%), February rainfall (11.9%), solar radiation (10.5%), annual rainfall (9.8%) and minimum temperature (5.6%). Some "clamping", where environmental variables and features are restricted to the range of values encountered during training after being detected outside of that range during testing, was detected during projection onto LGM surfaces, but was restricted to areas within the Southern Alps and Central Otago highlands, which would have been glaciated or above treeline during the LGM (Alloway *et al.* 2007). In the null model tests, the AUC score for *B. scutellaris* (0.885) ranked higher than all models drawn from random (AUC range 0.602-0.722) and from forests (AUC range 0.820-0.878).

Model results for *A. labralis* were consistent with those obtained in Chapter 2. The 10-fold cross-validation runs yielded an average AUC of 0.868 (sd 0.042, range 0.803-0.927), and performed significantly different than random at all but the lowest threshold for all runs. February temperature (36.3%) and October vapour pressure deficit (17.4%) remained the top two predictors of the species' presence, followed by February rainfall (15.5%), solar radiation (11.2%), annual rainfall (8.8%), annual temperature (5.5%) and minimum temperature (5.3%). Very little clamping was detected during LGM projection. In the null model tests, the AUC score for *A. labralis* (0.910) ranked higher than all models drawn from random (AUC range 0.609-0.747) and from forests (AUC range 0.844-0.904).

Projected modern distributions are nearly identical for *A. labralis* and *B. scutellaris*, particularly for the South Island, and are broadly congruent to the projected distribution for *E. lawsoni* (Figure 4.1). Notably, all three species are predicted to be

present in the central west coast with high probability, even though *B. scutellaris* is absent there. Adding the *Nothofagus*, Podocarpaceae and Myrtaceae layers as predictor variables lowers its probability of presence in this area but does not remove Westland from the projected range (Figure 4.1b). *Nothofagus* spp. became the top predictor for the distribution of *B. scutellaris* (28.5%), but ranked as high for *A. labralis* (27.9%). Podocarpaceae (2.4% and 4.0%) and Myrtaceae (1.5% and 3.4%) were not strong predictors of either species' distribution. All three vegetation types contributed less predictive power to the model for *E. lawsoni* than most climatic variables (6.2-7.4%).

Glacial refugia along the extended Karamea coast in the region identified by Alloway *et al.* (2007) and small refugia near the Haast River mouth were projected for all three species (Figure 4.1). For *A. labralis*, the 10-fold cross validation model is more conservative than using the 75%/25% training/testing data partitions (Figure 2.5), but projected refugia still extend south to central Westland; the key difference is elimination of the south Fiordland refugium, which was previously hypothesized with low probability. *Agyrtodes labralis* and *B. scutellaris* share a projected refugium between Nelson and Marlborough, and small refugia are projected in Marlborough for *E. lawsoni*—but with lower probability of presence. *Agyrtodes labralis* and *E. lawsoni* also share a projected refugium in Kaikoura, where *B. scutellaris* was projected to be absent.

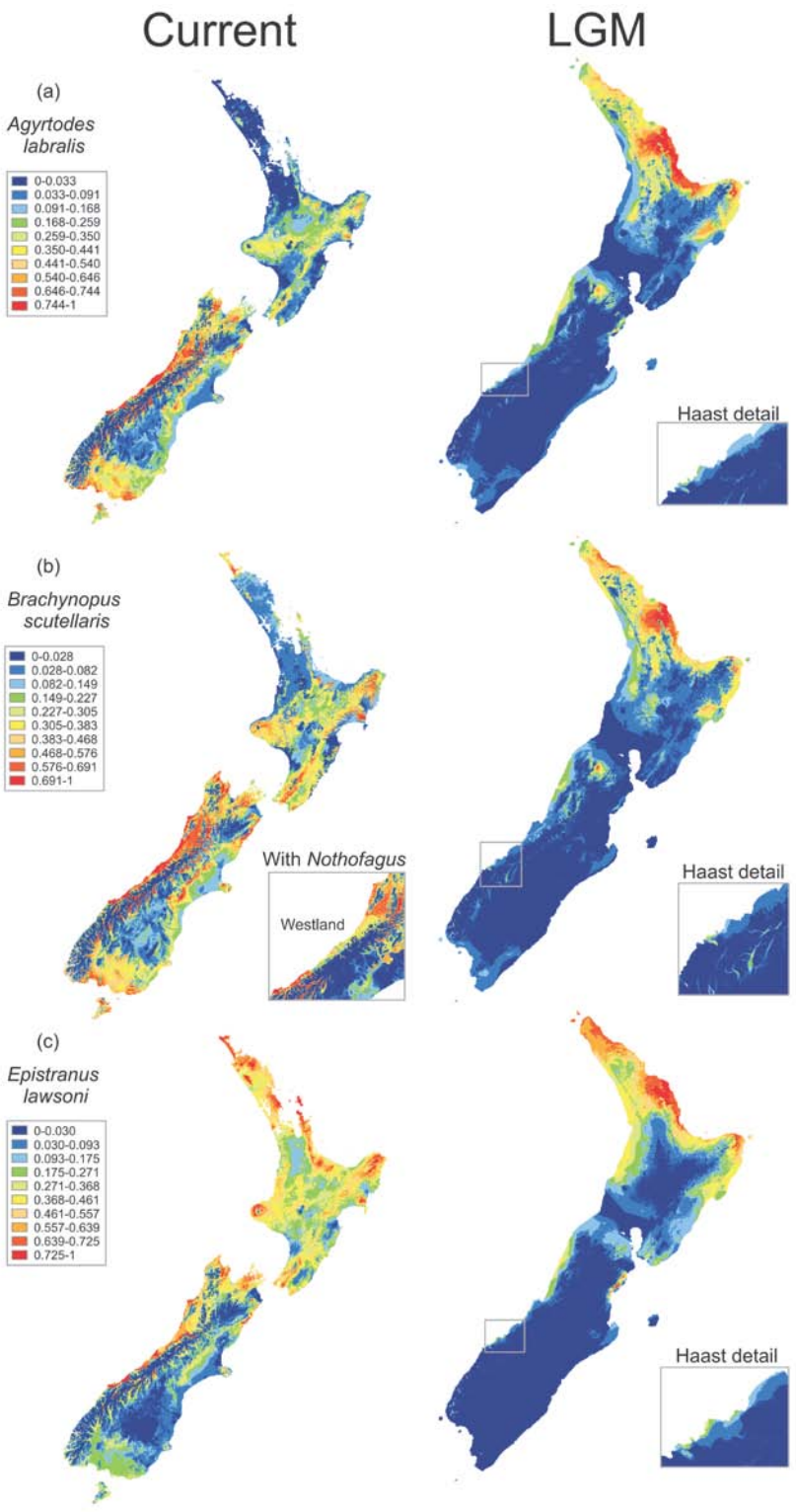

Figure 4.1. Ecological niche models for (a) *Agyrtodes labralis*, (b) *Brachynopus scutellaris* and (c) *Epistranus lawsoni*, averaged across 10 cross-validation runs. Current and LGM (c. 22,000 cal. yr BP) projections, and an enlargement showing the Haast refugium, are presented for each species. Modelling of the current distribution of *B. scutellaris* was repeated with additional vegetation layers, and an enlargement of central Westland is shown.

Results for *H. hystrix* scored lower than for the other species except *P. bakewelli* (Chapter 3). The 10-fold cross-validation runs yielded an average AUC of 0.758 (sd 0.042, range 0.705-0.83)—low for use in ecological applications (Pearce & Ferrier 2000). In the null model tests, the AUC score for *H. hystrix* (0.823) ranked higher than all points drawn from random (AUC range 0.614-0.726), but among the lowest compared to points randomly drawn from forests (AUC range 0.822-0.877). Jackknife tests indicated a negative average test gain for solar radiation and February rainfall, and inspection of test results for individual runs revealed erratic jackknife behaviour, with one or two variables with negative test gain appearing in multiple runs, but the variables with negative results were not consistent between runs. Refugia projections were broadly congruent between individual runs, but clamping was detected over substantial parts of the South Island during projection onto LGM surfaces, indicating the algorithm was "unsure" how to classify presence/absence over broad areas with the available data. Given the low AUC, the apparently poor fit of the predictor variables, and the extensive clamping, no projections are presented for *H. hystrix.* Due to poor model performance using only climatic variables for *H. hystrix* and *P. bakewelli*, and given the straightforward relationship between *H. hystrix*, *Nothofagus* and *Leptospermum* (Myrtaceae) relative to that between *B. scutellaris* and *Nothofagus*, vegetation variables were not used to model the distribution of these species.

4.3.2 Population genetics statistics

Total datasets for *B. scutellaris* and *H. hystrix* included 340 and 308 sequences, respectively. For *B. scutellaris*, 176 unique haplotypes were detected (Hd 0.9788), with 130 detected in one individual, 18 shared among individuals from the same locality, and

28 shared between localities. The two most abundant haplotypes were shared by 33 (eastern clade, below) and 23 (clade A, below) individuals, respectively. Mean uncorrected pairwise genetic distance (number of base pair differences) was 3.18% (corrected distance 0.0444), with maximum 6.36% (corrected distance 0.1691). For *H. hystrix*, 121 unique haplotypes were detected (Hd 0.9141), with 90 detected in one individual, 3 shared among individuals from the same locality, and 28 shared between localities. The most abundant haplotype was shared among 86 individuals and was distributed the length of the South Island's west coast, while the second most abundant haplotype, from Marlborough, was shared by only 13 individuals. Mean uncorrected pairwise genetic difference for *H. hystrix* was 0.89% (corrected distance 0.0094), with maximum 2.54% (corrected distance 0.0459). Tajima's *D* and Fu and Li's *F** and *D** were not significant for *B. scutellaris*; for *H. hystrix*, Tajima's *D* was also not significant, but Fu and Li's *F** and *D** had P< 0.02. Mean uncorrected pairwise genetic distance for *A. labralis* was 2.92% (corrected distance 0.0434), with maximum 4.70% (corrected distance 0.1503).

4.3.3 Coalescent phylogenies for *B. scutellaris* and *H. hystrix*

Bayes factors analyses strongly favoured the constant size model over the exponential growth model for both species. Posterior probabilities and coalescent dates shown were generated under the constant size model for *B. scutellaris* (Bayes Factor 152.6, S.E. +/- 0.13) and *H. hystrix* (Bayes Factor 1,356,485.101, S.E. +/- 0.117).

The coalescent topology constructed for *B. scutellaris* is consistent with that estimated by Leschen *et al.* (2008) with a subset of the data (Figure 4.2). Sister to the rest of the tree (posterior probability [pp] 1) is the Brady Creek clade, which includes all

haplotypes from the North Island and five locations along the Haast River. Coalescence of the root is estimated at 4.42 Ma (95% CI 3.01-6.07 Ma). Within this clade, the South Island lineages receive extremely low posterior support (pp <0.1) as a monophyletic group, and no well-supported North Island regional subclades are identified. Next is the Eastern Clade (pp 0.5847), which includes most of the eastern and southern South Island and diverged from the remaining lineages at approximately 3.62 Ma (2.40-4.93 Ma). The reciprocally monophyletic (pp 0.8600) A and B clades are largely distributed on the west coast, although both are present in the northeast South Island and clade A was detected in Southland and Stewart Island. Divergence of A and B was estimated at 2.77 Ma (1.80-3.76 Ma). Within clade A, the sequences from the northeast (Marlborough, pp 1) and southwest (Fiordland, pp 0.9283) form well-supported regional lineages, diverging from the rest at approximately 1.32 Ma (0.81-1.87 Ma) and 0.73 Ma (0.43-1.10 Ma), respectively. Remaining lineages are paraphyletic with respect to geography, with haplotypes from Southland and Stewart Island interspersed with those from Nelson and Buller. Within clade B, sequences from the northern South Island (Kaikoura, Marlborough, Nelson) form a well-supported group (pp 0.8815), with divergence from the rest estimated at 2.02 Ma (1.27-2.87 Ma). Most remaining sequences from the west coast fall into reciprocally monophyletic northern and southern clades (including the remaining Haast River haplotypes) straddling the *Nothofagus* gap, although this topology is not well-supported (pp <0.5), and excludes lineages from both regions, making them geographically paraphyletic.

Divergences are much shallower for *H. hystrix*, with relatively few well-supported regional clades (Figure 4.3). Coalescence at the root (pp 1) is between most Stewart Island haplotypes and the rest of the tree, and is estimated at 1.46 Ma (0.82-2.20 Ma). The next well-supported clade (pp 0.9215) includes all North Island sequences,

plus some from the northern South Island, and is reciprocally monophyletic to the remaining South Island sequences, diverging at approximately 0.94 Ma (0.56-1.36 Ma). Within this clade, South Island haplotypes from the east and west coasts do not form a single lineage, and divergence of North and South Island lineages is not strongly supported (pp <0.5). Very little phylogenetic or phylogeographic structure differentiates the remaining lineages, aside from a small, well-supported group including the northeast South Island and one locality in Fiordland (pp 0.7082). The remainder of this large clade spans the entire South Island and Stewart Island, and includes the species' most common haplotype.

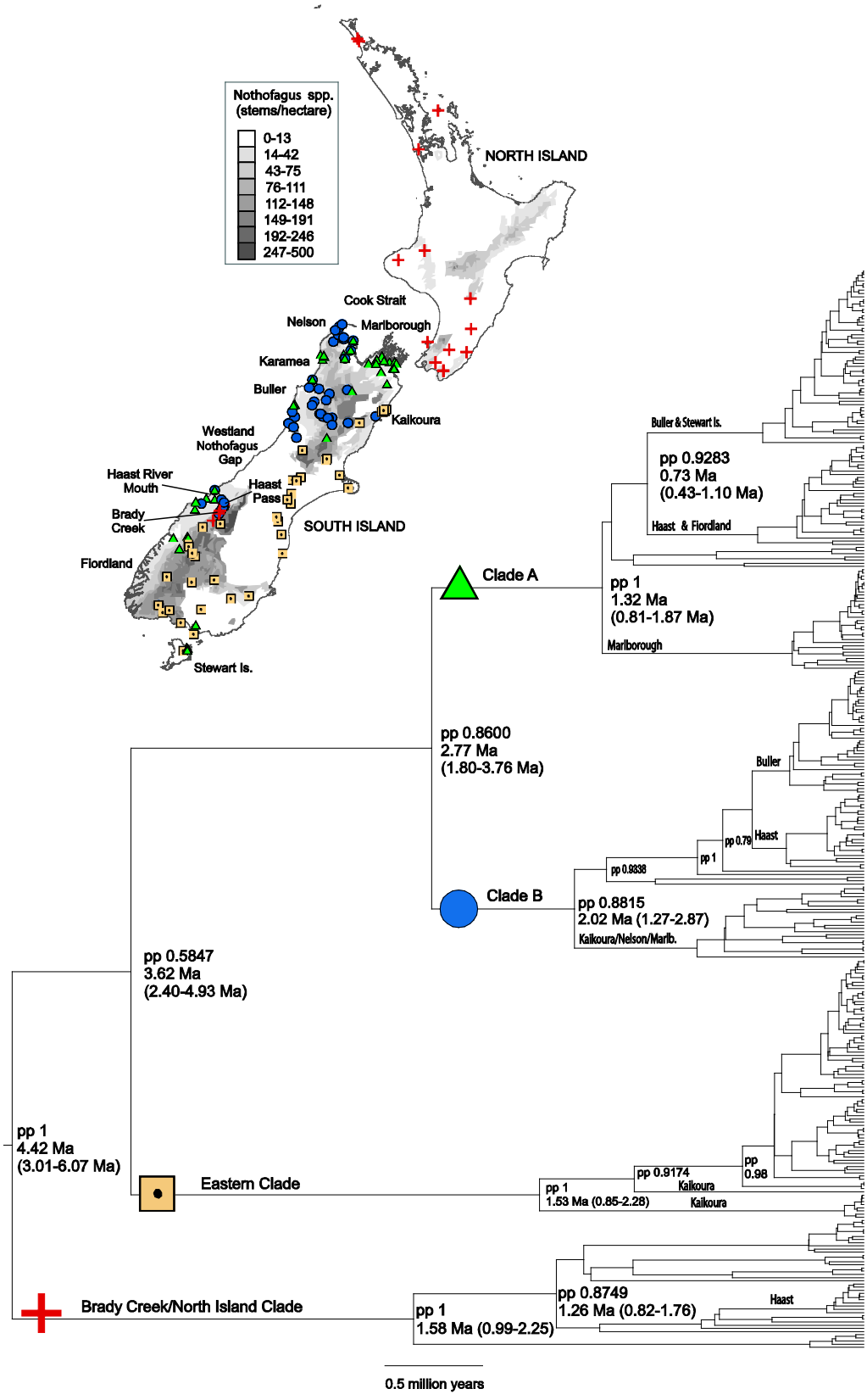

Figure 4.2. *Brachynopus scutellaris* populations sampled for molecular analysis and Bayesian coalescent tree with branch lengths drawn proportional to time (millions of years). Map shading indicates the distribution of *Nothofagus* forest (stems/hectare). Date estimates are given at selected tree nodes with pp>0.5.

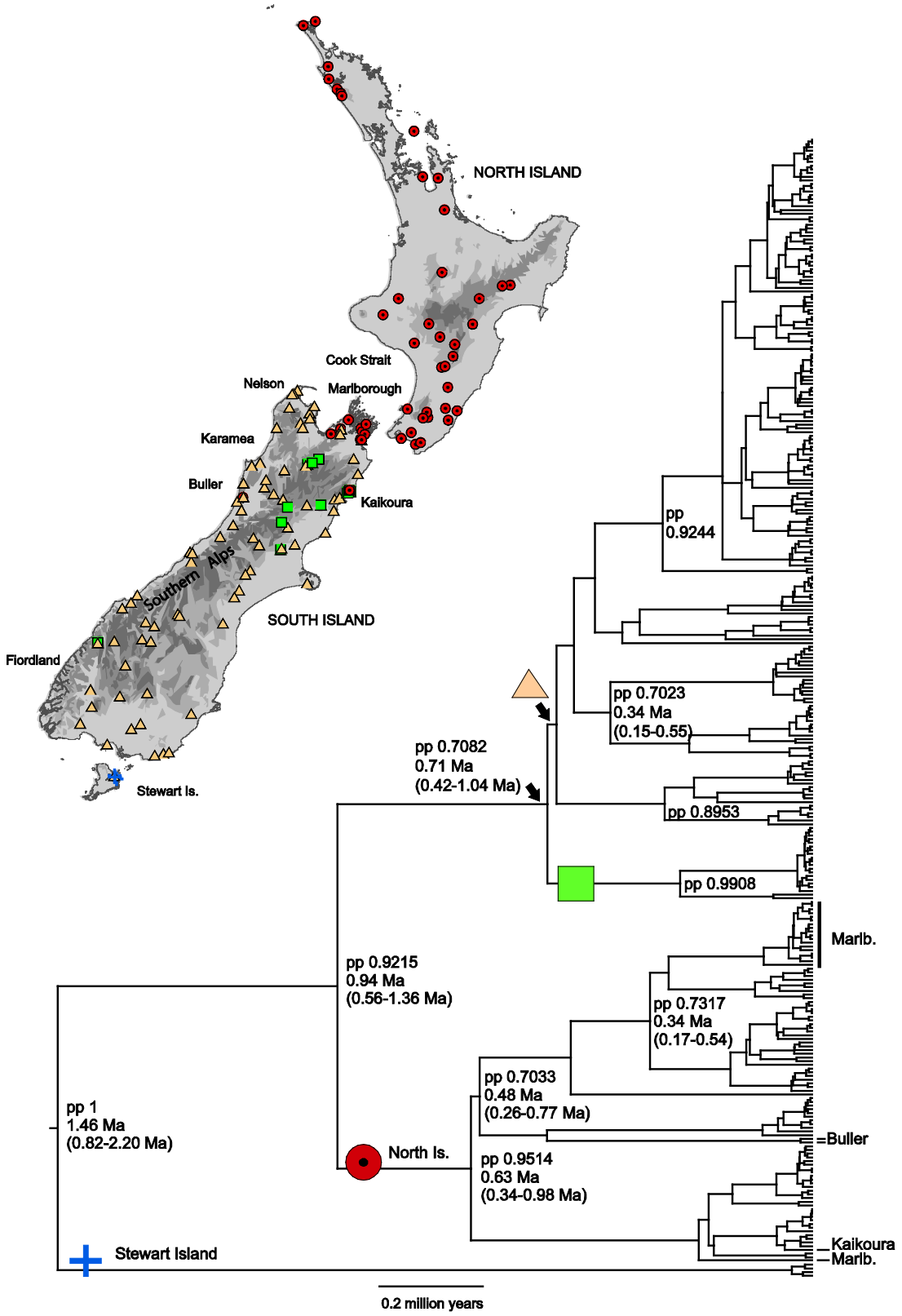

Figure 4.3. *Hisparonia hystrix* populations sampled for molecular analysis and Bayesian coalescent tree with branch lengths drawn proportional to time (millions of years). Map shading indicates topographic relief. Date estimates are given at selected nodes with pp>0.5. Labels at tree tips indicate South Island lineages within the North Island clade. Note that the "clade" indicated by the beige triangle is not well-supported.

4.3.4 Coalescent phylogeographic reconstruction

Bayes factor analysis of non-zero rates of location-state change (Table 4.1) for *A. labralis* revealed that each region is connected to nearly every other via significant non-zero rates, and no regions are more than two state-transitions apart. The highest Bayes factors (and most likely migration pathways) connected Nelson-Kaikoura, Buller-Canterbury, Haast-Westland, Haast-Southland, and Haast-Canterbury, with significant pathways moving both east-west and north-south (Figure 4.4). Phylogeographic ancestral state reconstruction yielded a scenario consistent with that outlined in Chapter 2, with the tree root placed in the northern South Island (Nelson, state probability [sp] 0.4283; or Kaikoura, sp 0.258). State probabilities for Westland and Southland fell within the lowest 5%, eliminating them as potential root locations. Southward dispersal along the west coast connected Buller and Haast, before eastern expansion in the last million years connected Haast to Southland, Canterbury and Westland and Buller to Canterbury (Figure 4.5).

Table 4.1. Bayes factor tests for significant (BF>3.0) non-zero rates of state-change between regions.

Species	Bayes factor	Locations
Agyrtodes labralis	Infinity	Haast x Southland
Agyrtodes labralis	213747.8	Buller x Canterbury
Agyrtodes labralis	3502.0	Westland x Haast
Agyrtodes labralis	1030.5	Nelson x Kaikoura
Agyrtodes labralis	610.3	Haast x Canterbury
Agyrtodes labralis	12.1	Westland x Southland
Agyrtodes labralis	11.2	Westland x Canterbury
Agyrtodes labralis	9.9	Westland x Kaikoura
Agyrtodes labralis	9.8	Buller x Haast
Agyrtodes labralis	8.8	Canterbury x Kaikoura
Agyrtodes labralis	8.6	Southland x Canterbury
Agyrtodes labralis	8.2	Haast x Kaikoura
Agyrtodes labralis	8.1	Buller x Westland
Agyrtodes labralis	7.7	Buller x Kaikoura
Agyrtodes labralis	7.5	Kaikoura x Southland
Agyrtodes labralis	7.2	Nelson x Buller
Agyrtodes labralis	7.0	Buller x Southland

Table 4.1 (*continued*).

Species	Bayes factor	Locations
Agyrtodes labralis	6.3	Nelson x Haast
Agyrtodes labralis	6.1	Nelson x Canterbury
Agyrtodes labralis	6.0	Nelson x Westland
Agyrtodes labralis	5.2	Nelson x Southland
Brachynopus scutellaris	814.8	Haast x Southland
Brachynopus scutellaris	523.9	Manawatu x Taranaki
Brachynopus scutellaris	95.2	Canterbury x Southland
Brachynopus scutellaris	22.1	Buller x Southland
Brachynopus scutellaris	13.2	Canterbury x Kaikoura
Brachynopus scutellaris	11.1	Nelson x Southland
Brachynopus scutellaris	8.2	Nelson x Kaikoura
Brachynopus scutellaris	4.3	Northland x Taranaki
Epistranus lawsoni	19628.8	Manawatu x Taranaki
Epistranus lawsoni	13653.8	Canterbury x Kaikoura
Epistranus lawsoni	2010.4	Haast x Southland
Epistranus lawsoni	96.7	Nelson x Canterbury
Epistranus lawsoni	46.5	Manawatu x Northland
Epistranus lawsoni	29.6	Buller x Haast
Epistranus lawsoni	20.4	Nelson x Manawatu
Epistranus lawsoni	5.9	Canterbury x Manawatu
Epistranus lawsoni	3.6	Buller x Southland
Epistranus lawsoni	3.4	Canterbury x Taranaki
Epistranus lawsoni	3.1	Nelson x Taranaki
Epistranus lawsoni	3.0	Southland x Kaikoura
Hisparonia hystrix	1168.9	Buller x Haast
Hisparonia hystrix	162.5	Manawatu x Taranaki
Hisparonia hystrix	77.6	Nelson x Buller
Hisparonia hystrix	51.7	Canterbury x Kaikoura
Hisparonia hystrix	16.7	Nelson x Canterbury
Hisparonia hystrix	5.0	Northland x Taranaki
Hisparonia hystrix	3.4	Canterbury x Southland
Pristoderus bakewelli	11473.6	Nelson x Buller
Pristoderus bakewelli	193.5	Manawatu x Northland
Pristoderus bakewelli	16.5	Buller x Haast
Pristoderus bakewelli	15.0	Nelson x Manawatu
Pristoderus bakewelli	3.5	Nelson x Kaikoura

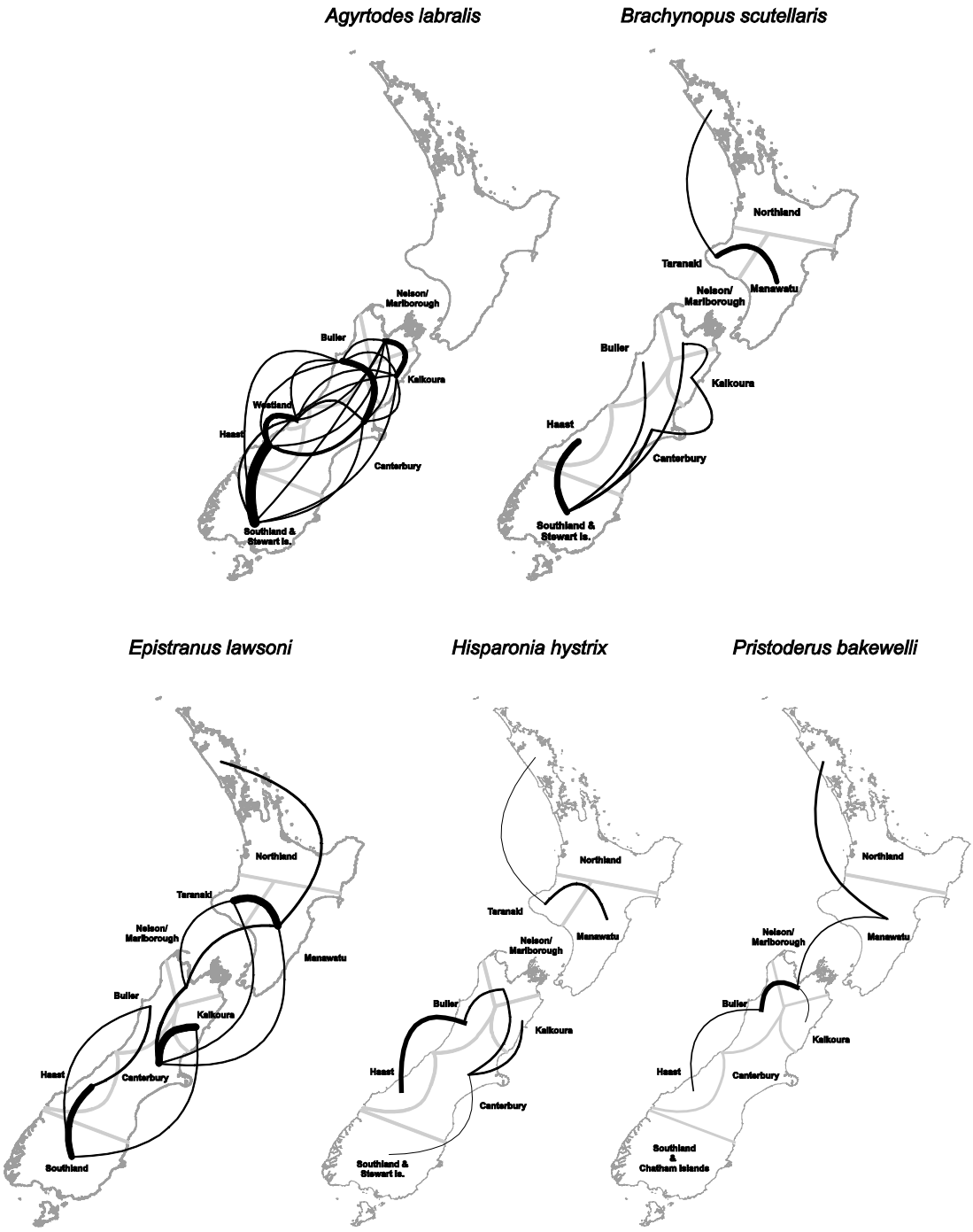

Figure 4.4. Migration matrices showing regions connected by significant (BF>3.0) non-zero rates of state-change for each species. Thickness of lines indicates the relative strength by which the rates are supported; Bayes factors for each connection can be found in Table 4.1.

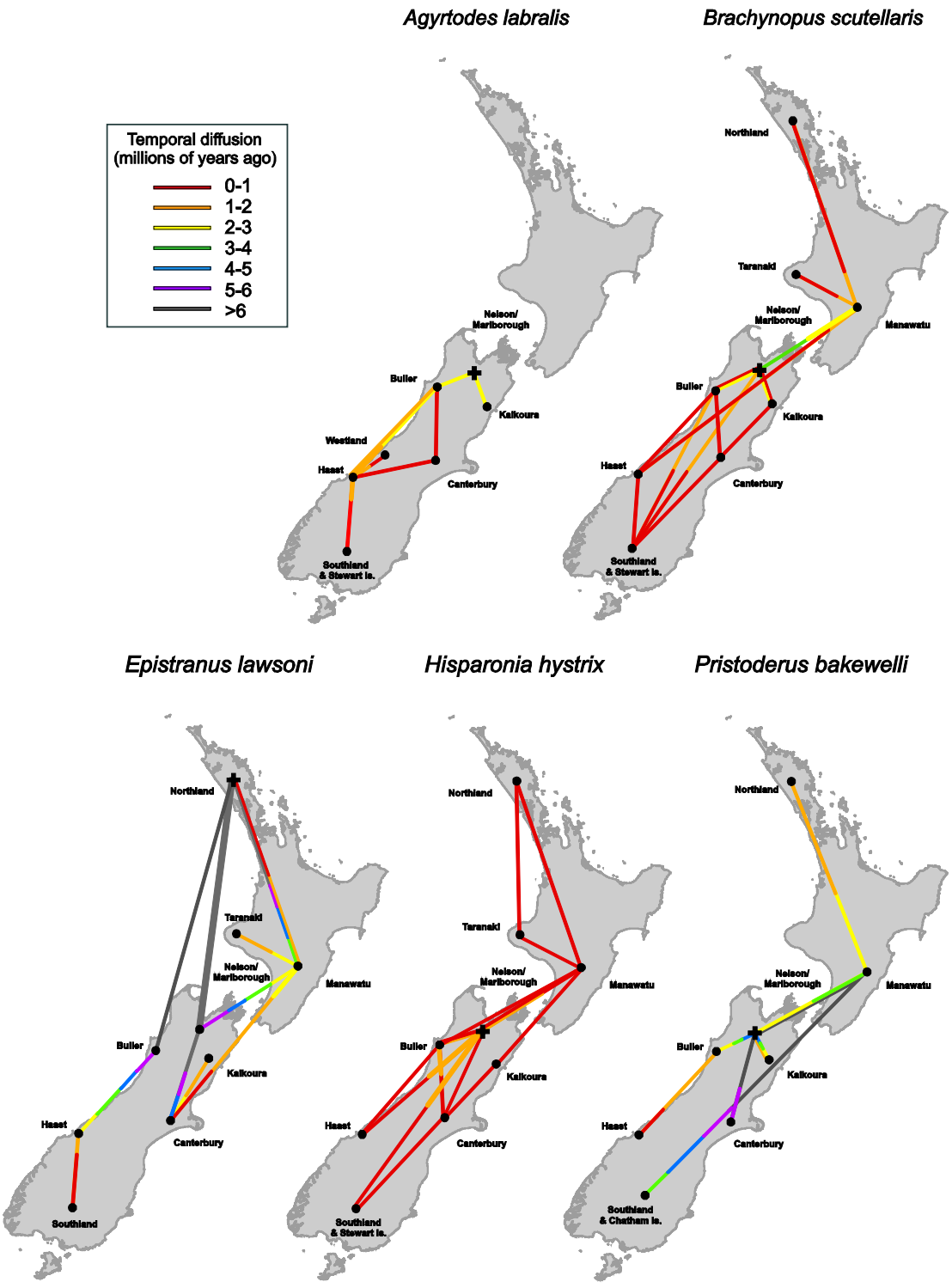

Figure 4.5. Temporal dynamics of spatial diffusion for each species summarised from ancestral state reconstruction of the geographic location for each tree node. Lines connecting locations indicate tree branches along which location transition occurs. Geographic mapping of the diffusion process is based upon locations which received the highest state probability for each node; in some cases the highest state probability was <0.5. Note that diffusion is bidirectional between some locations, indicated by thicker lines.

In contrast, Bayes factor analysis for the other species identified some regions with limited or no connectivity, particularly between coasts. For *B. scutellaris*, results indicated an absence of significant migratory routes along the west coast, with Nelson, Buller and Haast connected via Southland (Figure 4.4). Southland is also the hub for west-east migration, indicating that little, if any, direct migration occurs between coasts, as it does for *A. labralis*. The highest Bayes factors connected Haast-Southland and Taranaki-Manawatu, and no well-supported non-zero rates of state chance connected the North and South Islands. Placement of the root was ambiguous, with Nelson (sp 0.1792), Southland (sp 0.1736) and Haast (sp 0.1792) receiving similar state probabilities. Manawatu and Northland fell into the bottom 5%, strongly suggesting a South Island origin for *B. scutellaris*. Mapping of spatio-temporal diffusion of *B. scutellaris* haplotypes, treating Nelson as the root state, show Nelson, Manawatu and Buller connected first, with other regions occupied within the last 1 Ma (Figure 4.5).

The highest Bayes factors for *H. hystrix* connected Haast-Buller. Migratory pathways were predominately over short distances, with each region connected only to its nearest neighbour, with the exception of Canterbury-Nelson (Figure 4.4). No pathways connected the North and South Islands, and Nelson was the only hub connecting the east and west coasts of the South Island. Placement of the root was also ambiguous for *H. hystrix,* with Nelson (sp 0.1890), Southland (sp 0.1746), Kaikoura (sp 0.1669) and Canterbury (sp 0.1666) all receiving similar state probabilities, although Taranaki and Northland fell into the bottom 5%, strongly suggesting a South Island origin. *Hisparonia hystrix* has a shallower root than the other species, and mapping of spatio-temporal diffusion treating Nelson as the root indicates a complex network of spatial seeding, with only Nelson and Buller occupied > 1Ma (Figure 4.5).

For *E. lawsoni*, the highest Bayes factors were between Taranaki-Manawatu, Canterbury-Kaikoura, and Haast-Southland (Figure 4.4). The only migratory pathway linking the eastern and western South Island with significant non-zero state transition rates was via Southland, as for *B. scutellaris*. Ancestral state reconstruction for *E. lawsoni* using fewer regions than in Chapter 3 did not result in any significant changes over the previous results, with the South Island's west coast populations descending directly from Northland. Most South Island locations, except for Nelson and Canterbury, had state probabilities in the lowest 5%, further supporting a North Island root location. For *P. bakewelli*, Canterbury and Southland were not connected to any other regions and migratory pathways were over relatively short distances, with each region connected only to its nearest neighbour. The highest Bayes factors were between Nelson-Buller and Northland-Manawatu (Figure 4.4). Using fewer region-states greatly improved phylogeographic estimation for *P. bakewelli*, with most of the previously unassigned nodes (Figure 3.5) placed in Nelson (state probabilities >0.5). Root placement was still ambiguous, with Nelson (sp 0.3556), Manawatu (sp 0.2904) or Buller (0.1623) as the most likely locations, with Haast and Canterbury effectively eliminated (<5%). Events spanned by the coalescent trees for both *E. lawsoni* and *P. bakewelli* largely predated the Pleistocene and particularly the LGM (Chapter 3), with root coalescence several million years older than for the other three species (~25 Ma and ~10 Ma, respectively).

4.4 Discussion

Results for all five species yielded a complex picture of temperate forest community evolution. *Agyrtodes labralis* yielded phylogeographic patterns consistent

with Pliocene mountain orogeny and isolation in the modelled coastal LGM refugia, followed by west-east colonization in the Holocene (Chapter 2). *Brachynopus scutellaris* shared many of the same modelled refugia (Figure 4.1), but gene flow in this species was largely north-south rather than west-east, interrupted by the Westland *Nothofagus* gap. Strikingly deeper coalescence of *E. lawsoni* and *P. bakewelli* lineages suggested older geographic influences, including the closing Manawatu Strait and uplift of the Southern Alps (Chapter 3). In contrast, *H. hystrix* yielded relatively little genetic diversity with recent intraspecific divergence dates, suggesting a constricted geographic range during the Pleistocene followed by rapid expansion.

Each of the five species shared some features of its results, such as individual migration routes or projected refugia, but no general species-level patterns, such as flighted vs. unflighted, log/leaf litter vs. arboreal, or ancient vs. recent intraspecific divergence dates, were detected. While projected glacial refugia were shared among the three species whose distributions were successfully modelled, the spatial and temporal dynamics of genetic diffusion and many of the migratory pathways leading from these refugia were strikingly different. Using multiple genetic loci might reveal different evolutionary patterns, and the disadvantages and risks associated with using single-locus datasets are discussed in Chapters 2-3, but similar ENMs among species make a strong argument for these refugia and the migratory pathways connecting them. Because the beetles are serving as proxies for the temperate forest ecosystem, the sum of patterns across multiple species is more informative for understanding community evolution than would be a highly-resolved, multi-locus phylogeny for a single taxon, as this allows differentiation between shared vs. species-specific evolutionary trends.

4.4.1 Coalescent Phylogeography

Statistically rigorous coalescent methods are fast becoming a staple in the phylogeography literature and are regarded as a vital step toward the inference of fully objective biogeographic scenarios using genetic data (Hickerson *et al.* 2010). Among the most popular are methods which test specific biogeographic hypotheses through coalescent simulation (e.g., Carstens & Richards 2007) or simultaneous vicariance across a common biogeographic barrier (e.g., Leaché *et al.* 2007). Less common are coalescent methods which use ancestral state reconstruction to map historical dispersal patterns (e.g., Lemey *et al.* 2009), although they have been addressed under likelihood statistical frameworks (e.g., Lemmon & Lemmon 2008). As in the latter example, the present study features taxa distributed across a continuous landscape, while empirical systems used to demonstrate *a priori* hypothesis testing often feature single-barrier vicariant scenarios (e.g., habitat disjunction; Carstens & Richards 2007). Given New Zealand's recent tectonic history, potential vicariant barriers are numerous and some (e.g., Southern Alps, Pleistocene glaciers) overlap in space and time. An additional complicating factor is that the projected South Island glacial refugia are now largely submerged, meaning most, if not all, genetic samples were drawn from localities colonized post-LGM, not the refugia themselves. These features of the study system make it less amenable to explicit hypothesis testing than to methods which do not require *a priori* identification of historical events—although assigning collection localities to region-states in this context does carry some implicit *a priori* assumptions.

The advantage of using coalescent ancestral state reconstruction is that it provides a full probabilistic inference of phylogeography from the data by simultaneously estimating the location and date of each node (Lemey *et al.* 2009) while

accounting for the stochastic nature of evolution, which sets it apart from previous reconstruction methods requiring fully resolved phylogenies (e.g., Lemmon & Lemmon 2008). This allows identification of tree branches on which state transitions (migration events) occur and mapping of the spatial diffusion of lineages. Genealogical patterns do not always reflect demographic and evolutionary processes, and the Bayes factor tests for significant non-zero rates of state transition identify important migratory pathways, replacing subjective tree interpretation with results which can be mapped and compared among species. A key disadvantage is that increasing the depth of the root (relative to other nodes) increases uncertainty of the root state, resulting in similar posterior probabilities for all states, but the separate non-zero rate analyses compensate for this by identifying locations predominant throughout the phylogeny, and measuring the relative importance of these migratory hubs by quantifying state transitions through them (Lemey *et al.* 2009). For the five Coleoptera, the precision of spatio-temporal diffusion mapping (Figure 4.5) may have been reduced by low state probabilities at deeper nodes, reversibility of state change (assuming migration in both directions) and broad confidence intervals on divergence date estimates for some species (Chapter 3). This makes the topology-independent migration matrices particularly useful for identifying well-supported patterns of gene flow and comparing patterns among taxa with different intraspecific divergence dates. A future extension of this method might be to use the migration matrices to inform hypotheses for coalescent simulations by narrowing down competing hypotheses in topographically diverse environments.

The migration matrices (Figure 4.4) indicated several patterns in common, although none were shared by all five species. For *A. labralis*, *B. scutellaris* and *E. lawsoni*, strongly supported pathways connected Haast, where all three had projected refugia, with Southland, from which all three were absent during the LGM, suggesting a

common dispersal route. All species but *A. labralis* had extremely limited genetic diffusion between the South Island's east and west coasts. While this could be related to gradual expansion from refugia on either coast, the sharing of those refugia by *A. labralis*, which subsequently crossed from west to east, suggests that the Southern Alps were a more potent migratory barrier for the other species. For *E. lawsoni*, where deep coalescent dates are hardest to reconcile with recent events like the LGM, the absence of east-west migration indicates consistency between genetic and ecological methods, with the west coast populated from western refugia and the east populated from refugia in Kaikoura and potentially the Marlborough Sounds and lower North Island. In the three species with lineage coalescence <5 Ma, the root and earliest branches of the tree are placed in the northern South Island, although for *B. scutellaris* and *H. hystrix* a southern South Island origin could not be statistically ruled out. Similar root state probabilities between Nelson/Marlborough and Southland (the second highest for both species) may be related to the divergent haplotypes detected only on Stewart Island (*H. hystrix*) or haplotypes shared between Stewart Island and Buller (*B. scutellaris*).

Strikingly different spatial and temporal patterns were also detected among species. The majority of well-supported connections for *B. scutellaris*, *E. lawsoni*, *H. hystrix* and *P. bakewelli* were between neighbouring regions. Mapping the spatial diffusion of these species through time did not indicate strong directionality and for *B. scutellaris* and *H. hystrix*, in particular, branches moved contemporaneously in multiple directions. Lemey *et al.* (2009) detected a similar pattern in their rabies virus example and interpreted the relationship between the tree and migration matrix as different simultaneous migration events in various directions, with most migrations over short ranges between neighbouring regions. In contrast, spatio-temporal diffusion in *A. labralis* occurred primarily northwest to southeast, consistent with the post-glacial

scenario described in Chapter 2, in which Canterbury and Southland were colonized from west coast refugia after diffusion through the Southern Alps. The best-supported migration pathways are consistent with this scenario, and no locations are more than two state transitions away from any other, suggesting that dispersal pathways are relatively unhindered by geographic barriers in this species.

4.4.2 Convergent refugia from divergent histories

Ecological niche modelling projected broadly congruent glacial refugia for three species with distinctly different evolutionary histories, suggesting that results for individual species are correct. The relationship between projected refugia and phylogeographic patterns is relatively straightforward for *A. labralis*, and the two western refugia (Karamea and Haast) were hypothesized for *B. scutellaris* based on proposed glacial origins for the *Nothofagus* gap (Leschen *et al.* 2008), but for *E. lawsoni*, with its ancient divergence dates and heightened intraspecific diversity, detecting patterns from the relatively recent LGM would have been impossible without incorporating ENMs. All three species had refugia indicated near Karamea, as in Alloway *et al.* (2007), but agreement on the Haast refugium, combined with strong migratory pathways connecting Haast with Southland for all three species (see below) indicate that this small refugium may have been very important for postglacial forest colonization of southern New Zealand. The Nelson/Marlborough and Kaikoura refugia were each detected by two species and would have contributed to forest colonization of the east, particularly for taxa for which the Southern Alps are a dispersal barrier.

How the measured climatic variables interacted with physiology and ecology to result in the projected range restrictions was not directly measured by this experiment,

but some hypotheses can be drawn by comparing the beetle results with two stick insects, which are, to date, the only other New Zealand invertebrates for which ENMs were developed. For the three Coleoptera, minimum temperature ranks relatively low in importance, below the other temperature and both rainfall variables. In contrast, the stick insects, for which refugia were largely restricted to the North Island, had minimum temperature as the top-ranked variable (explaining 57-64% of model fit; Buckley *et al.* 2009, 2010). This is likely related to the differences between insulated dead wood and leaf litter habitats vs. the exposure of the canopy. Both rainfall variables made relatively low contributions to the stick insect models but were more important for the beetles; this may be related to ability of forest litter to maintain enough moisture for sufficient fungal growth. Interestingly, intraspecific radiations in the flightless stick insects are much more recent than in the hardier *E. lawsoni*, which would have maintained a broader but more fragmented geographic range (more refugia over broader geographic extent) during the LGM.

Failure of the ENMs for *H. hystrix* and *P. bakewelli*, strictly interpreted, indicates that the niche of each species is driven by factors other than the tested climatic variables. For *H. hystrix*, these additional factors are somewhat obvious given its dependence on the sooty mould ecosystem, which is driven by feeding and honey-dew secretion by large scale insects not restricted to tall forest tree species like *Nothofagus* (Carlton & Leschen 2007). Phylogeographic results for *H. hystrix* indicate little geographic structure (Figure 4.3) and recent spatial diffusion in multiple directions (Figure 4.5), and significant P-values for Fu and Li's *F** and *D**—combined with a non-significant Tajima's *D**—potentially implicate population expansion driving an excess of rare alleles (Fu & Li 1993). These factors, plus the shallow genealogy for this species relative to the others, suggest a limited range for *H. hystrix* during the LGM

with later dispersal, but may reflect climatic restrictions imposed upon the scale insects or sooty mould, not the beetle itself. For *P. bakewelli*, drivers of its geographic distribution are less obvious and little is known about the ecology of this species. Combined with poor genetic resolution of historical connections to the southern South Island, presumably resulting from the limited number of sequences relative to the other species, making predictions about LGM refugia for *P. bakewelli* is difficult, although older divergence dates and early seeding of the South Island (Figure 4.5) suggest that South Island refugia would have been utilized.

4.4.3 Westland *Nothofagus* gap revisited

For *B. scutellaris*, nearly tripling the number of sequenced individuals and broadening the geographic sampling base over Leschen *et al.* (2008) did not substantially alter the phylogenetic results, reaffirming the pattern of the nearly parallel phylogenetic structure of the west coast clades and the relationship of Haast Pass lineages to the North Island (Figure 4.2). The *Nothofagus* gap-spanning topology of clades A and B is modified slightly from Leschen *et al.* (2008); clade B maintained a distinct split between Buller and Haast lineages, although the split is not well-supported (pp <0.5), preventing accurate divergence date estimates. In clade A, the Haast populations form a well-supported monophyletic group, diverging from Buller in the mid-Pleistocene, but the Buller populations are closely related to individuals from Southland and Stewart Island, and the relationship of these regions to each other is paraphyletic. The pattern of two clades straddling the *Nothofagus* gap (instead of separate clades north and south of the gap) is difficult to interpret in light of this peculiar relationship and the absence of well-supported migratory pathways connecting

either across or around the gap (via an eastern location) or between Buller and any northern regions (Figure 4.4). However, the relationship between Buller and Southland/Stewart Island might reflect a widely-distributed coastal haplo-group which remained largely undetected south of the gap because of the inaccessibility of coastal Fiordland. Sampling from this area might shed light on this unexpected phylogenetic and migratory connection.

Phylogenetic relationships between Haast and the North Island, also initially identified by Leschen *et al.* (2008), are poorly resolved, with the Haast lineages nested within the North Island clade ($pp<0.5$). The absence of strong migratory routes connecting Haast (or any of the South Island) with the North Island suggests that the phylogenetic link represents a rare historic dispersal event (≤ 1 Ma; Figure 4.5), although retraction of a previously widespread lineage cannot be conclusively ruled out. This geographic connection is therefore difficult to place within a historical context, although a similar pattern was detected in an estuarine fish and was attributed to Plio-Pleistocene glaciation (Hickey *et al.* 2009).

Ecological niche modelling also failed to elucidate the relationship between *B. scutellaris* and *Nothofagus*, which share the central Westland disjunction but are not co-distributed throughout their range in the east coast, Stewart Island or the North Island. The current projected distribution for *B. scutellaris* indicates that maintenance of this disjunction is not climatically driven, which concurs with similar findings for *Nothofagus* (Leathwick 1998), and *A. labralis* and *E. lawsoni*, which would also have been absent from parts of Westland during the Pleistocene, have filled the gap (although projected refugia for these species extended further south than for *B. scutellaris*, resulting in less gap to fill). Incorporating *Nothofagus* as a predictor in the ENM lowered the beetle's probability of presence in Westland, but *Nothofagus* also became

the top predictor for *A. labralis*, explaining about 30% of model-fit for both species. Clearly the mechanisms driving both the disjunction and the related phylogenetic patterns are beyond the scope of what this study is able to detect.

An important question rising from the *Nothofagus* gap discussion is that given the current absence of *B. scutellaris* from apparently suitable habitat on the west coast and *A. labralis* from the North Island, how can we determine whether these species utilized the projected refugia? For *A. labralis*, Cook Strait (and its predecessor the Manawatu Strait) may have represented an impassable boundary, and suitable North Island habitat during the LGM was restricted significantly north of the land connection, possibly preventing northward migration. The current distribution of *B. scutellaris* is harder to explain, but fossil evidence places the species at Westport, abutting the Karamea refugium, during the LGM (Burge & Shulmeister 2007). Strong concordance of refugia for *A. labralis* with the genetic data and concordance of both species' refugia with that of *E. lawsoni*, for which no species-climate disequilibrium is suspected, suggests accuracy of the predictions.

4.4.4 Glacial refugia and forest community evolution

In spite of shared LGM refugia and similar modern distributions, these five beetles do not appear to share the broadly similar population structure which would make them evolutionary cohorts (*sensu* Carstens & Richards 2007). Phylogenetic structure, spatial diffusion of each species through time, and important migratory connections between populations are very different, in spite of the shared bioclimatic niche detected in three species. While the three flighted species have histories implicating relatively recent events, like Pliocene mountain orogeny and Pleistocene

glaciation (e.g., Chapter 2), the flightless species recall much earlier periods in New Zealand's topographic evolution. This may be a result of their limited dispersal capabilities, in which results of population fragmentation take longer to "drift" away with fewer opportunities for gene flow between neighbouring populations; a similar difference in phylogeographic structure between flighted and unflighted beetles was noted by Papadopoulou *et al*. (2009) in the Aegean archipelago. The population dynamics of each species relative to the projected refugia suggest that their evolutionary trajectories have repeatedly intersected in space and time, but they are not travelling as an intact community.

In spite of the obvious differences among species, a clearer picture of LGM forest dynamics is emerging. Predictions of convergent refugia among species with different evolutionary histories are a strong indicator of where forests survived and how they colonized their current range. It is most likely that forests expanded in multiple directions from the projected refugia (McGlone 1985), with attendant species following along as they could, either through mountain passes or along either flank of the Southern Alps. While there may have been some post-glacial migration from the North Island, the sum of the dynamics among species suggest that refugia located in the South Island were most important in generating the detected genetic structure. Results are also broadly consistent with those for other species: the Kaikoura refugium may have been shared by the stick insect *Argosarchus horridus* (White) (Buckley *et al.* 2009), and phylogenetic results for the cicada *Kikihia subalpina* (Hudson) suggest it was restricted to the northern South Island and utilized available refugia on either side of the Southern Alps (Marshall *et al.* 2009). Therefore, to the Karamea refugium detected by Alloway *et al.* (2007), the insect phylogeographic data suggest additional refugia at Haast, Nelson/Marlborough and Kaikoura. Future studies of additional taxa are expected to

yield new insights into the relative importance of these refugia to the forest biota, and into the roles of concerted vs. individual climate response in recent evolutionary patterns.

What does this mean for identifying forest refugia and using individual species to detect ecosystem dynamics? Sullivan *et al.* (2000) explicitly tested whether communities of species shifted in concert in response to glacial cycles, or whether species and populations responded independently, and found the answer to be somewhere in between. This is certainly the case with the New Zealand beetles, in which divergent migratory routes around different vicariant barriers have repeatedly converged upon similar geographic distributions. While some elements of forest ecosystems would have moved together, no single piece was a mirror image of modern forests (Stewart *et al.* 2010), which is why detailed studies of multiple distantly related taxa are needed to accurately address ecosystem evolution (Carstens *et al.* 2005). This bottom-up, species-driven approach to community evolution also emphasizes the uniqueness of each ecosystem's reaction to climate change, with the response to global climate phenomena largely determined at the local level.